



## Chemical Methodologies

Journal homepage: <http://chemmethod.com>



### Review article

# Different Interface Engineering in Organic Solar Cells: A Review

Oluwatobi O. Amusan<sup>a</sup>, Hitler Louis<sup>b, c</sup>, Saud-uz-Zafar<sup>c</sup>, Adejoke T. Hamzat<sup>a</sup>, Dass M. Peter<sup>d</sup>

<sup>a</sup> Department of Chemistry, University of Ilorin, Ilorin, Kwara State, Nigeria

<sup>b</sup> Department of Pure and Applied Chemistry, Faculty of Physical Sciences, University of Calabar, Calabar, Cross River State, Nigeria

<sup>c</sup> CAS Key Laboratory for Nanosystem and Hierarchical Fabrication, CAS Centre for Excellence in Nanoscience, National Centre for Nanoscience and Technology, University of Chinese Academy of Sciences, Beijing, China

<sup>d</sup> Department of Chemistry, Faculty of Physical Sciences, Modibbo Adama University of Technology, Yola, Nigeria

#### ARTICLE INFORMATION

Received: 27 September 2018  
Received in revised: 12 November 2018  
Accepted: 05 February 2019  
Available online: 11 March 2019

DOI: [10.22034/chemm.2018.150142.1096](https://doi.org/10.22034/chemm.2018.150142.1096)

#### KEYWORDS

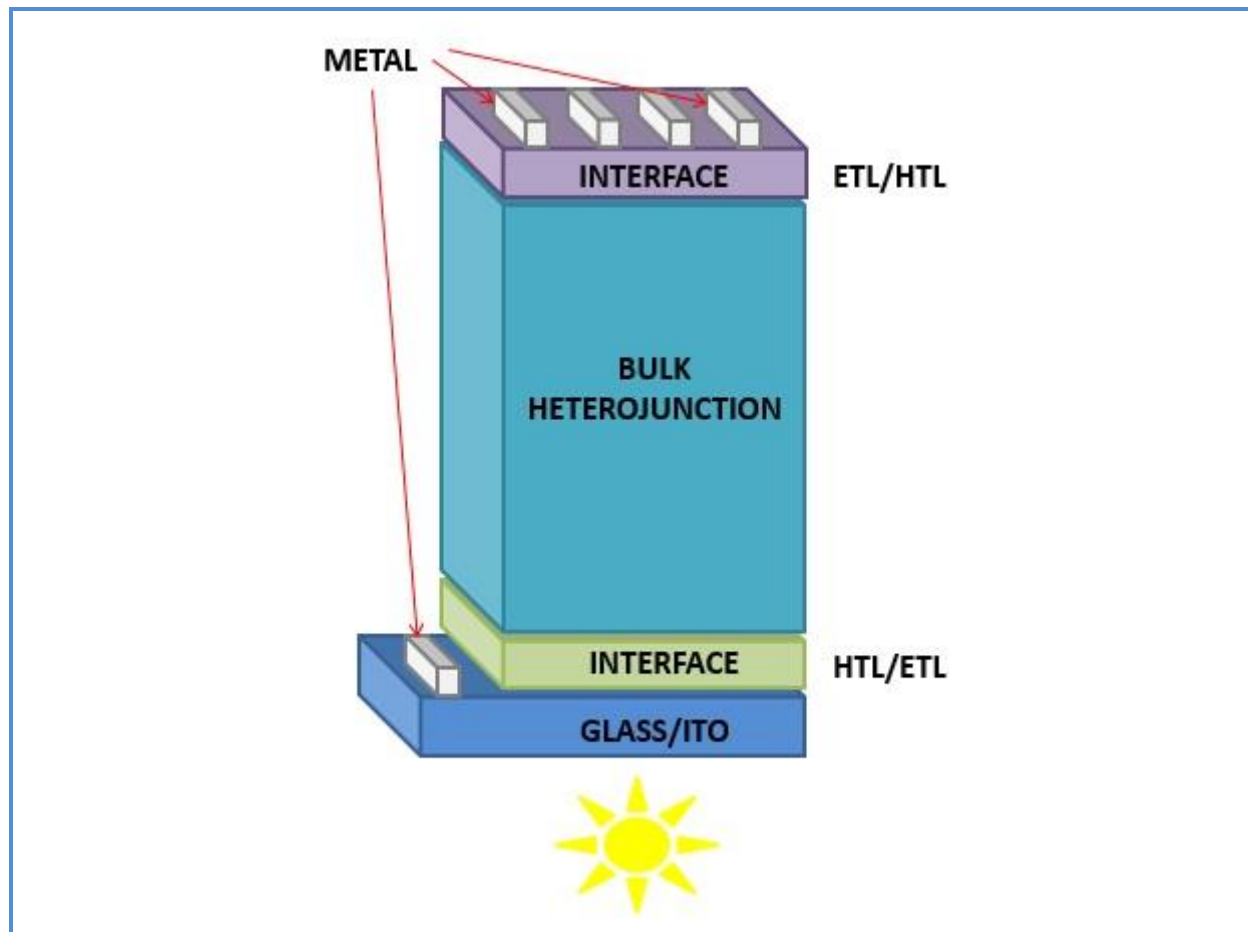
Power conversion efficiency (PCE%)  
Bulk heterojunction (BHJ)  
Interfacial layer  
Electron transport layer (ETL)  
Hole transport layer (HTL)  
Indium tin oxide (ITO)

#### ABSTRACT

The global quest for reliable sources of energy has led to the development of Organic solar cells (OSCs)/ Organic photovoltaics (OPVs). Over the past few years, they have shown great potentials and use as low cost devices for conversion of solar energy. OSCs are designed from different interface layers from different materials which form a major determinant for their energy conversion efficiency. The recent development in the modifications in design and engineering of these interface materials have shown increased power conversion efficiency (PCE%) of Organic photovoltaics. Interface materials are conductors, semiconductors or non-conductors which provide selective contact for carriers, determine polarity and acts as protective layers. This review discusses different materials which are used as interface materials as well as their structure and engineering.

\*Corresponding author: E-mail: [philipmonday2018@nanocr.cn](mailto:philipmonday2018@nanocr.cn), CAS Key Laboratory for Nanosystem and Hierarchical Fabrication, CAS Centre for Excellence in Nanoscience, National Centre for Nanoscience and Technology, University of Chinese Academy of Sciences, Beijing, China

## Graphical Abstract



## Introduction

Organic solar cells (OSCs) are electronic devices which are used for the conversion of solar energy to electricity using low cost organic materials [1]. The organic materials used for the design of OSCs are characterized by their low cost of production leading to the wide recognition and great interest in the design of OSCs which are considered as inexpensive source of renewable energy among other sources of energy [2-5]. OSCs as compared to other solar converters are lightweight flexible devices with less adverse environmental effects which are fabricated from organic solution which can be processed at high throughput [6-7].

Organic solar cells can be made from active polymer and fullerene based electron acceptor as the illumination of the setup by visible light which leads to the movement of electron from the polymer to the fullerene acceptor [2]. The organic molecule is sandwiched between two contacts occurring as either single or multilayer as shown in Figure 1. Depending on the nature of material used in

OSCs, the band gap can be adjusted to facilitate the conversion of low energy photons to direct electricity. Conjugated systems are commonly used as active materials. The band gap between the valence band (highest occupied molecular orbital, HOMO) and the conduction band (lowest unoccupied molecular orbital, LUMO) of organic material is considered in the choice of the right conjugated system. When an organic material absorb photons, there is an excited state (exciton or electron hole pairs) generated which is held together by electrostatic attraction. Effective fields which are set up by creating a heterojunction between two different materials, break up the excitons causing the movement of electron from the absorber (donor) to the receptor (acceptor) molecule. The basic process in the conversion of photons to electricity in OSC is highlighted below:

- (a) Photons fall on the device and then they are absorbed by the donor and excitons are generated.
- (b) The excitons diffuse into interface of donor- acceptor set up and are split as carriers.
- (c) The split carriers are transported into corresponding electrodes.
- (d) Photo generated carriers are extracted to the electrodes by interface layers.

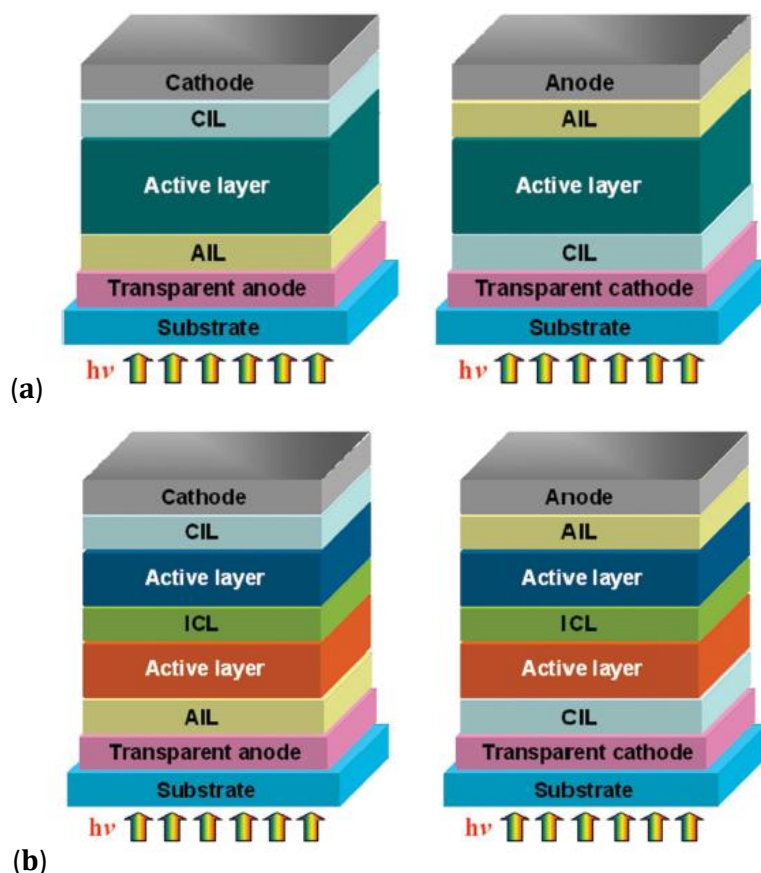


**Figure 1.** (a) Conventional and inverted single junction organic solar cell (b) Conventional and inverted bilayer organic solar cell

From the early work on OSCs fabrication, increment in the efficiencies has been a major subject of interest for research. Power conversion efficiency (PCE %) expressed as short circuit current ( $J_{SC}$ )  $\times$  open circuit voltage ( $V_{OC}$ )  $\times$  electrical fill-factor (FF)/ incident optical power density ( $P_{Max}$ ) which is a major factor to be considered in any circuit. OSCs have experienced increased efficiencies up to 12% in recent development in the engineering of materials [8-11]. The improved PCE % of OSCs are attributed to the improved engineering leading to the application of effective electron donor and acceptor as well as the novel interface materials in their design [12]. Therefore, improved activity of choosing an appropriate material as interface is a very important factor to be considered, as different materials possess different PCE % [13]. Interface materials adjust the band gap between the active layer and the electrodes forming a selective contact for carriers and acts as optical spacers. The first part of this review will discuss about the interface engineering in OSCs, the electron transport layer and hole transport layer will be discussed in the later part with broad insight into the various materials used in their design and their synthetic methodology.

### Interface engineering in organic solar cells

Interface materials are a major component of organic solar cells. They are placed between the photoactive layer, *i.e.*, donor and acceptor materials, and the electrode materials as shown in Figure 2. Interfaces play a vital role in the maintenance of proper contact between photoactive layers in an organic solar cell. They are placed between donor and acceptor materials and the electrode. They are used to achieve ohmic contact at the organic/metal interface. They form a selective contact preventing the formed charge carriers and excitons from recombining at the electrodes thereby increasing cell efficiency. Among other roles of interface materials, they also act as protective layers.

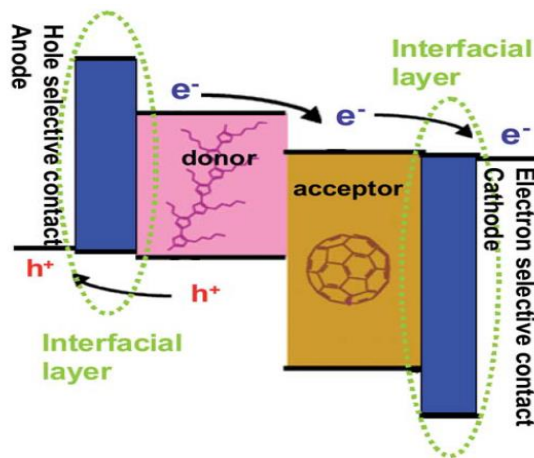


**Figure 2.** Schematic illustration of an organic solar cell with interface materials

The power conversion efficiency of OSCs is as a result of four processes that occur with the device; generation of excitons, diffusion of excitons to an electron donor/acceptor interface, generation of holes as a result of charge separation and transport and collection of charge carriers. Apart from these four processes, the quality of the interface materials is another crucial factor to be considered because they are responsible for facilitating good contact which aid the afore mentioned processes. A typical OSC has a light absorbing bulk heterojunction (BHJ) between two electrodes [4]. They play important roles in determining the efficiency of OSCs. Due to the major role played by the interface materials in determining the efficiency of OSCs, several works have been done recently to further raise their power conversion efficiency making interface engineering the major point of attention [14-24].

In order to compare and improve the efficiency of OSC using different buffer layer deposited on the indium tin oxide (ITO) anode, Bernede [25] used bathocuproine (BCP) in a multilayer heterojunction structure *i.e.*, Glass/ITO/BF/ED/C<sub>60</sub>/BCP/Alas interface at electron donor/acceptor junction. He observed that anode bilayer showed improved power conversion efficiency reducing the hole extraction barriers. Dazheng Chen and Chunfu Zhang [26] investigated the effect on PCE% of OSC by modification of cathode layers and ITO free electrodes. For the inverted organic solar cell where a poly (3-hexylthiophene-2,5-diyl): [6,6]-phenyl C<sub>61</sub> butyric acid methyl ester [P3HT:PCBM] blend was used, aqueous solution at low temperature was adopted to deposit zinc oxide interlayer. When the tin oxide was heated above 80 °C, PCE% of over 3.5% was observed whereas a flexible setup based on poly (ethylene terephthalate) substrate showed a PCE% of 3.6%. Other materials such as ultrathin Ca modifier (~1 nm) at AZO/Ca/organic interface showed 3% while 2 nm MoO<sub>3</sub> interlayer for silver anode showed and improved value of 2.71%. The design of the interface was represented in Figure 3 as Glass/ITO/ZnO/P3HT:PCBM/MoO<sub>3</sub>/Ag, with the zinc oxide precursor coated on a nitrogen dried ITO-coated substrates achieving a thickness of 10 nm. Next, the P3HT:PCBM(1:0.8 wt% in 1,2-dichlorobenzene) solution was spin-coated on ZnO in a nitrogen filled glove box achieving a thickness around 100 nm. Finally, the MoO<sub>3</sub>(8 nm)/Ag (100 nm) anode was thermally evaporated through a shadow mask and the resulted devices have an active area of 10 mm<sup>2</sup>. The fabricated OSC have a structure shown in Figure 3, where P3HT:PCBM acts as the photoactive layer, the ZnO film act as electron transport layer and hole blocking layer. MoO<sub>3</sub> also acts as the hole transport layer and electron blocking layer, with ITO and Ag playing the roles of cathode and anode respectively.

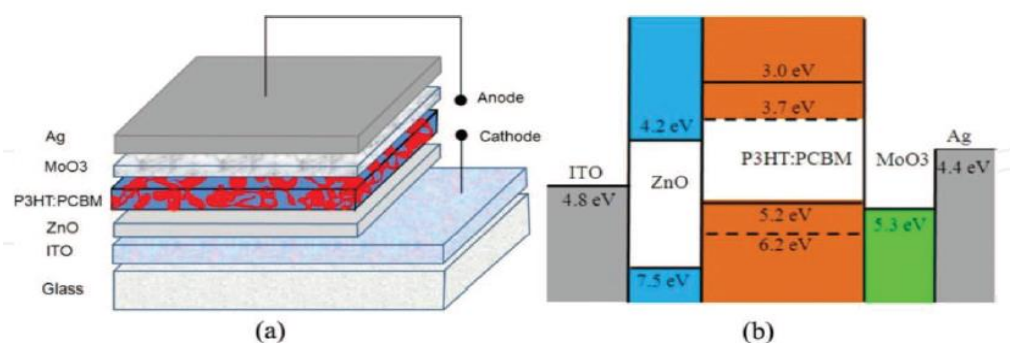


**Figure 3.** (a) Device architecture (b) Energy levels of materials

Kunal Borse investigated phenyl- $C_{71}$  butyric acid methyl ester ( $PC_{70}BM$ ) as interface between ZnO based electron transport layer (ETL) and photoactive layer comprised of Poly[4,8-bis(5-(2-ethylhexyl)thiophen-2-yl)benzo[1,2-b;4,5-b']dithiophene-2,6-diyl-alt-(4-(2-ethylhexyl)-3-fluorothieno[3,4-b]thio-phene)-2-carb-oxylate-2-6-diyl)] ( $PTB7-Th$ ): $PC_{70}BM$  as shown in Figure 4. The interface engineering modification adopted prevented electron hole recombination at the interface and PCE% from 6.65 to 7.74% was observed. The OSC was designed in an inverted geometry having a structure ITO/ZnO/ $PC_{70}BM$ / $PTB7-Th:PC_{70}BM$ /MoO<sub>3</sub>/Ag having  $PC_{70}BM$  as an interlayer between the electron transport layer and the photoactive layer. An additional V-grooved textured PDMS films was placed on the backside of OSC substrates which raised PCE% to 9.12%. In order to confirm the effect of the interfacial material used and the additional PDMS, several works were carried on this as shown in Figure 4 [26]. In another work [27], he compared performance of poly[4,8-bis(5-(2-ethylhexyl)thiophen-2-yl)benzo[1,2-b;4,5-b']dithiophene-2,6-diyl-alt-(4-(2-ethylhexyl)-3-fluorothieno[3,4-b]thio-phene)-2-carb-oxylate-2-6-diyl)] ( $PTB7-Th$ ):  $PC_{70}BM$  OSC in an inverted geometry with zinc oxide, a bilayer ZnO/ $Ba(OH)_2$  and a nanocomposite ZnO: $Ba(OH)_2$  as ETL as shown in figure 5. It was observed that the PCE% of the devices with the ZnO/ $Ba(OH)_2$  and ZnO: $Ba(OH)_2$  nanocomposite as ETL is better than in devices with only ZnO as ETL.

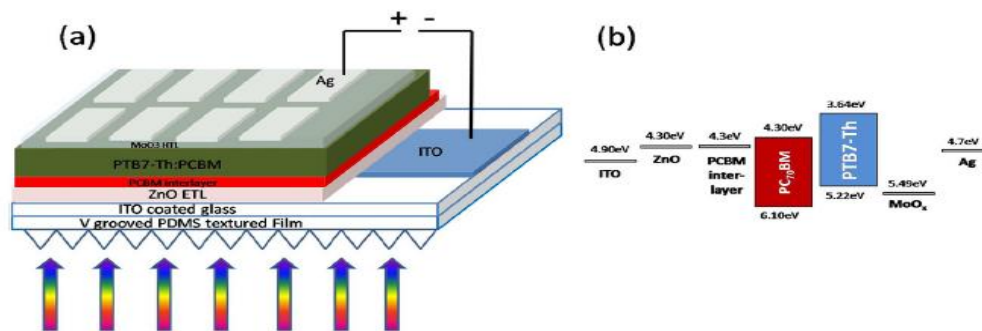


**Figure 4.** (a) Device architecture (b) Energy levels of materials

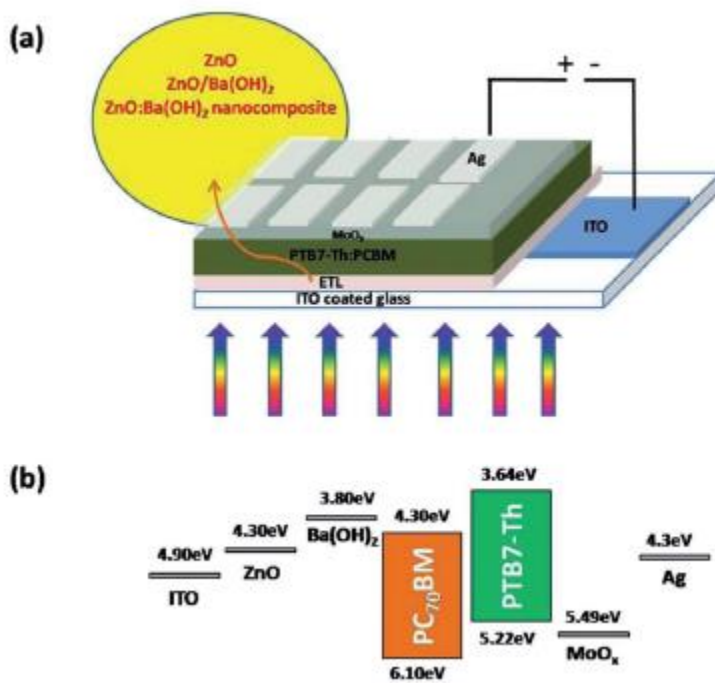


Figure 5. (a) Device architecture (b) Energy levels of materials

Another work reported the design of ITO/molybdenum oxide (MoO<sub>x</sub>)/boron subphthalocyanine chloride (SubPc)/bathophenanthroline (BPhen)/Al in fabrication of OSC as shown in Figure 6. Here C<sub>60</sub> was replaced with SubPc, the device output (PCE%) greatly improved from 3.38% to 5.03% by inserting a thin organic hole transport layer of rubrene on the interface between MoO<sub>x</sub> and SubPc to achieve an arrangement ITO/MoO<sub>x</sub>/rubrene/SubPc/BPhen/Al thereby preventing the exciton and charge combination at the anode [28].

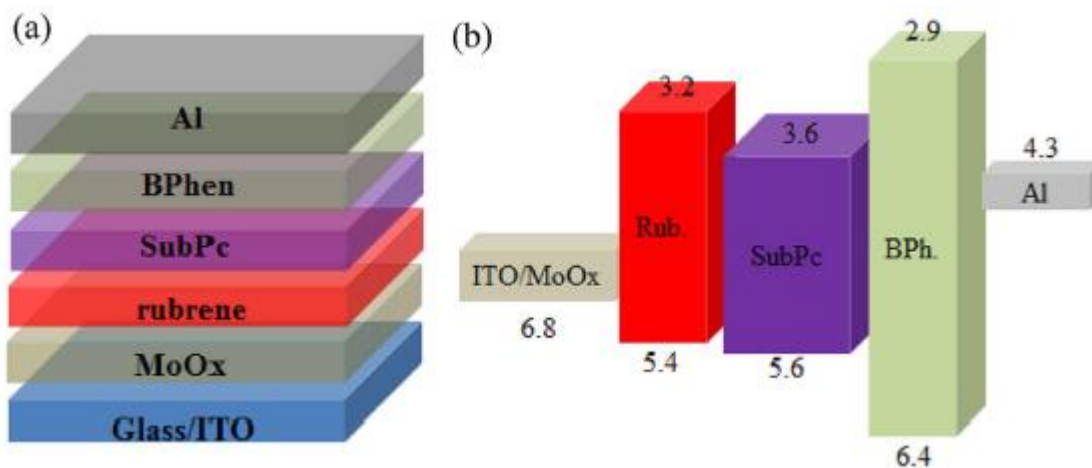
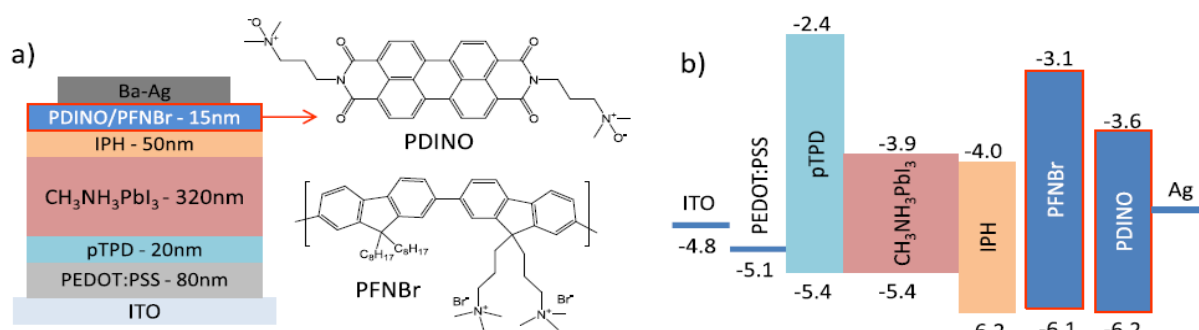


Figure 6. (a) Device architecture (b) Energy levels of materials

Lidon et al., [29] compared the efficiency of two different materials (perylene diimide derivative and a conjugated polyelectrolyte) as an interface between the fullerene ETL and the Ag electrode. The fabrication was made in the order ITO/PEDOT:PSS/poly TPD/MAPbI<sub>3</sub>/IPH/PDINO or PFNBr/Ba-Ag or Ag as shown in Figure 7. Both materials showed improved PCE when compared with the conventional organic solar set up.



**Figure 7.** (a) Device architecture with molecular structures of the PDINO and PFNBr (b) Energy levels of materials

Another innovative bilayer cathode interlayer (CIL) with a nanostructure consisting of in-situ thermal reduced graphene oxide (ITR-GO) and poly[(9,9-bis(30-(*N,N*-dimethylamion)propyl)-2,7-fluorene)-alt-2,7-(9,9-dioctyl) fluorene] (PFN) has been fabricated as an interface material in OSC with the structure ITO/bilayer CILs/PTB7:PC<sub>71</sub>BM/MoO<sub>3</sub>/Ag as shown in Figure 8 [30]. This bilayer ITR-GO/PFN CIL is processed by a spray-coating method with facile in-situ thermal reduction. It showed a good charge transport efficiency and less charge recombination, which led to an improved PCE from 6.47% to 8.34% for Poly({4,8-bis[(2 ethylhexyl)oxy]benzo[1,2-b:4,5-b0]dithiophene-2,6-diyl}{3-fluoro-2-[(2 ethylhexyl)carbonyl]thieno[3,4-b]thiophenediyl} (PTB7):[6,6]-phenyl-C<sub>71</sub>-butyric acid methyl ester (PC<sub>71</sub>BM)-based OSCs making ITR-GO/PFN CIL a good interface material.

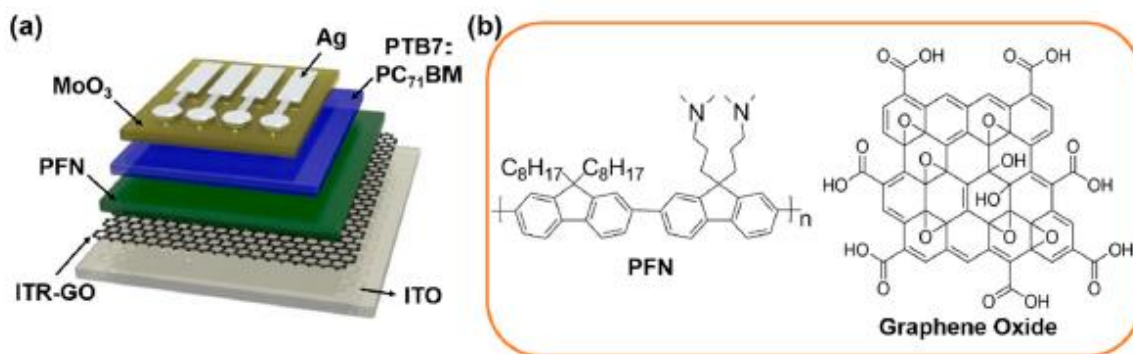


**Figure 8.** (a) Device architecture (b) Chemical structures of the materials



In a bid to study the role of interface materials, PBDTTPD-COOH interfacial layer was used on PEDOT:PSS in organic solar cells with the structure ITO/PEDOT:PSS/(PBDTTPD:COOH)/polymer:PC<sub>71</sub>BM BHJ/LiF/Al/Mg as shown in Figure 9 [31]. PBDTTPD-COOtBu was synthesized and unprotected to yield PBDTTPD-COOH and used in fabrication of ITO/PEDOT:PSS/PBDTTPD-COOH/BHJ/LiF/Al/Mg. Treatment of the standard ITO/PEDOT:PSS electrode with CHCl<sub>3</sub>:DMSO increased PCE% from 5.6% to 6.1%. Modification of the interface to include PBDTTPD-COOH interfacial layer further raised the PCE to 6.4% making it a good interface material.

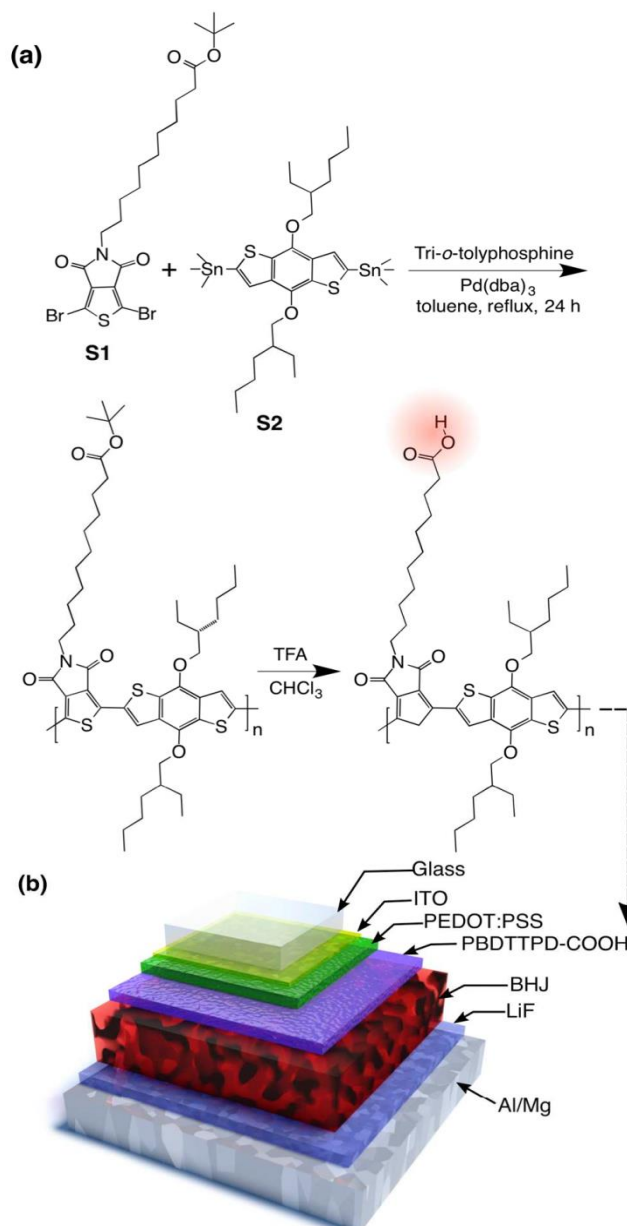


**Figure 9.** (a) Synthesis of acid-functionalized PBDTTPD polymers (b) Forward device architecture: ITO/PEDOT:PSS/(PBDTTPD:COOH)/polymer:PC<sub>71</sub>BM BHJ/LiF/Al/Mg

Shang-Chou *Chang* et al. [32] investigated Graphene (GN) doping concentration and annealing temperature in blended poly (3-hexylthiophene) and [6,6]-phenyl C<sub>61</sub> butyric acid methyl ester P3HT/PCBM) with GN (P3HT/PCBM /GN) based organic solar cells (OSC) fabrication as shown in Figure 10. In their study, they observed that P3HT/PCBM/GN based OSC can be efficiently increased by 3 wt% GN doping and 120 °C annealing, after experimenting and comparing PCE% values at different annealing temperature, as it showed good crystallization enabling easy transport of charge carriers.

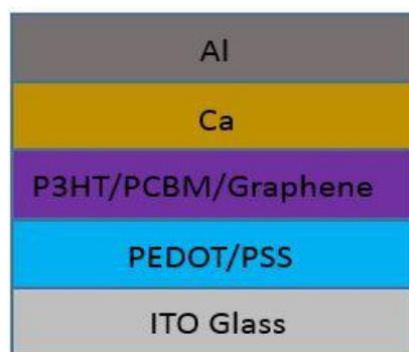


**Figure 10.** Device architecture with P3HT/PCBM/GN

Another novel work reported the fabrication of fuller pyrrolidine derivative, named FPNOH as an efficient electron-collecting (EC) layer for inverted organic solar cells (i-OSCs) with the active blend layer of poly[(4,8-bis(2-ethylhexyloxy)-benzo(1,2-b:4,5-b')-dithiophene)-2,6-diyl-alt-(4-(2-ethylhexyl)-3 fluorothiopheno[3,4-b]thiophene)-2-carboxylate-2,6-diyl]: [6,6]-phenyl-C<sub>71</sub>-butyric acid methyl ester (PTB7:PC<sub>71</sub>BM) as shown in Figure 11 [33]. It was observed that it showed a higher PCE% of 8.34% when compared to sol-gel ZnO reference device making it a good choice for interface in OSCs.

A lot of achievement reported in a lot of interface engineering towards a better power conversion efficiency in OSCs, more research is still in progress with many more to come as the whole world moves towards a sustainable source of power and energy.

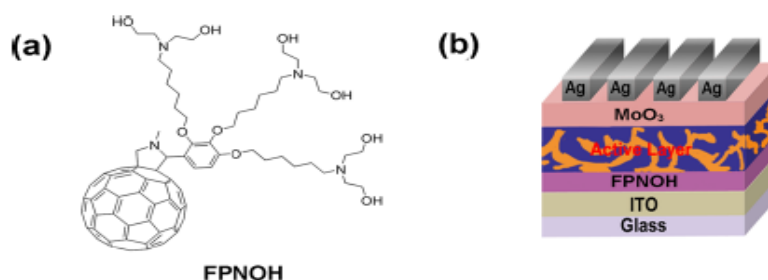


**Figure 11.** (a) Chemical structures of the neutral fuller pyrrolidine EC interlayer used in solar cell fabrication; (b) The inverted device architecture

### Electron transport layer (Etl)/ hole transport layer (Htl)

The working principle of OSCs have been discussed in the earlier part of this review to follow the basic principle of absorbing of light leading to the generation of excitons and separation of these excitons into two opposite charge carriers which are then transported within the device to different electrodes for the conversion and generation of current. The active materials in OSC apart from the interface materials, which have been discussed in the above section, also includes the special materials which acts as electron/ hole transport materials as shown in Figure 12. The ETL and HTL which are either applied in a conventional or inverted structure are vital to the PCE of OSCs as they are responsible for the initial stage of any activity which involves the absorbing of light. HTL and ETL both increase the charge extraction efficiency and reduce the bimolecular recombination at the electrodes in organic solar cells.

ETL and HTL among other major qualities are expected to be transparent, chemically stable with good electrical properties.

Here, we will discuss the recent advances in materials used as ETL and HTL as well as their synthetic methodology.

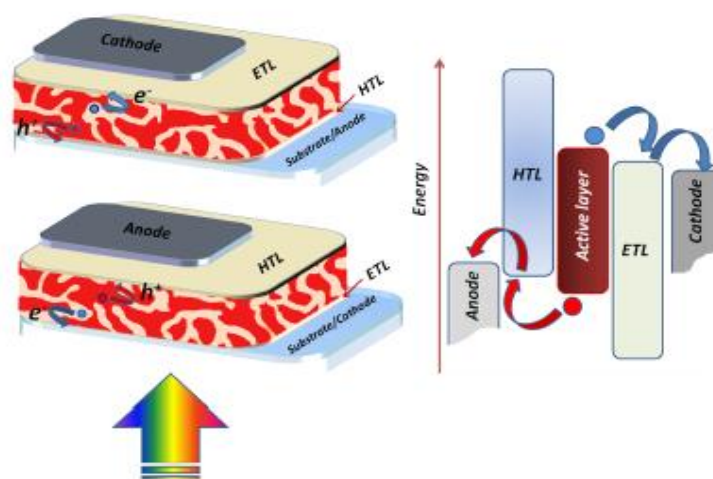


**Figure 12.** Schematics of OSC showing hole transport layer (HTL) and electron transport layer (ETL)

### Electron transport layer (ETL)

One major function of ETL is the transport of electrons. They are expected to be transparent as well as have a good transport property. Recent developments in design and fabrication of ETL materials have given rise to the following materials.

### Zinc oxide (ZnO)

Zinc oxide is one of the major materials used as ETL in OSCs because of its high electron mobility. *Irfan Ullah et al.* [34]. Processed ZnO through sol-gel method as an efficient ETL for iOSC (Inverted Organic Solar Cell). It was introduced in P3HT:PCBM based OSC to facilitate the transport of electrons as shown in Figure 13. The ZnO was treated at different temperature to ensure complete removal of solvent and dryness. Further modification to ZnO was done by doping it with low work function materials to further improve their improved PCE [35, 36].



**Figure 13.** Device architecture

### ZnO:Ba(OH)<sub>2</sub> nanocomposites

In order to improve the efficiency of solar cells by the engineering of the ETL, ZnO:Ba(OH)<sub>2</sub> nanocomposite has been developed to replace ZnO commonly used in ETL [28]. It was observed that the ZnO:Ba(OH)<sub>2</sub> nanocomposites have low work function as compared to ZnO. The ZnO solution was mixed with a corresponding volume of Ba(OH)<sub>2</sub> solution and fabricated using the setup in Figure 5. ITO substrate was coated with the nanocomposite until a film is achieved. The substrate were then annealed at 200 °C to remove the excess solvents, and then dried in a nitrogen filled glove box. Their current density, voltage values were measured with other characterizations. With this set up, it was observed that a PCE% was raised to 20% higher than devices with only ZnO as ETL due to increase in  $J_{sc}$  and FF recorded by the devices with ZnO:Ba(OH)<sub>2</sub> nanocomposites.

### Titanium dioxide (TiO<sub>2</sub>)

Titanium dioxide has been used in ETL processed by sol-gel, spin coated on ITO substrate [37]. Prepared ITO coated glass substrate was cleaned and the thin films of TiO<sub>2</sub> was coated. Titanium isopropoxyde was added to a mixture of methanol and isopropanol under continuous stirring at 80 °C using acetic acid as a catalyst to prepare the titanium oxide which was doped on ITO for better performance as ETL.

### **Fullerene**

An efficient fullerene based electron transporting material, C<sub>60</sub>N, *N,N*-trimethyl-1-(2,3,4-tris(2-(2-methoxyethoxy)ethoxy)phenyl)dimethanaminium monoadduct iodide salt (LT-S9079) [38]. The material was made by a slot die coating system with the PEDOT:PSS aqueous coated. The LT-S9079 solution made up with methanol was deposited on the substrate and allowed to stand for some time. The coating was made to be relatively thick enough to standard. Upon coating, they were annealed in the oven over a range of temperature and then to nitrogen filled glove box to get rid of excess solvent.

### **Caesium iodide**

Caesium iodide has been used in interface engineering of electron transport layer [39]. The efficiency of caesium iodide as well as the effect when it is coupled with ZnO was studied. Both the CsI and ZnO were spin coated on the pre-treated substrate to form an acceptable electron transport layer which was annealed in oven and placed in nitrogen glove box for complete removal of solvent. It was observed that the use of CsI coupled with ZnO showed an improved PCE of 12% as compared to the conventional ZnO.

### **Other novel materials**

Other materials which were fabricated for use as electron transport layer has been reported in relevant studies [40-44]. They were observed to have good electron transport mobility as well as chemical stability which are required of materials used in electron transport layers in OSCs.

### **Hole transport layer (HTL)**

To obtain a good performance in organic solar cells, the introduction of hole transport layer between the organic material and the electrode is proven as a way out of the poor performance of OSCs. Up to date the commonly used materials, in addition to the commonly used ones (PEDOT:PSS, NiO<sub>x</sub>, MoO<sub>x</sub>, CuSCN) include doped PEDOT:PSS, CuSeCN, V<sub>2</sub>O<sub>5</sub>, Graphene oxide.

### **PEDOT:PSS**

Poly(3,4-ethylenedioxythiophene):poly(styrenesulfonate) (PEDOT:PSS) colloidal particles have been the most commonly used material as hole transport layer [45]. Due to its good transport property, apart from the early work where it was used, recent modifications have been done to it to increase the outputs in OSC. MoO<sub>3</sub> [45], pentacene [46] have been used as efficient doping materials to increase the efficiency of PEDOT:PSS. The pre-treated substrates are being spin coated with MoO<sub>3</sub> and pentacene and placed in oven and subsequently in nitrogen filled glove box to remove excess solvent.

**CuSeCN**

Recent advances in the field optoelectronics have identified copper (I) selenocyanate as a suitable material in HTL [47]. It was prepared by addition of potassium selenocyanate (KSeCN) to a solution of excess copper (I) ions, freshly prepared by the reduction of copper (II) sulfate ( $\text{CuSO}_4$ ) by sodium thiosulfate ( $\text{Na}_2\text{S}_2\text{O}_3$ ). The resulting CuSeCN compound was “grayish-white” in color and sparingly soluble in water, in agreement with Söderbäck’s work. The synthesized CuSeCN was dissolved in diethyl sulphide and the resulting solution was spin coated on a pre-treated substrate plate to a visible layer which was used. CuSeCN was observed to show good electron transport property, hence its use as HTL.

 **$\text{V}_2\text{O}_5$** 

Vanadium pentoxide has been investigated as a recent development in materials used in HTL [48]. The effect of different diluents on the electrical properties of the vanadium oxide films was investigated using a roll coater. The pre-treated substrates are being spin coated with  $\text{V}_2\text{O}_5$  and pentacene and placed in oven and subsequently in nitrogen filled glove box to remove excess solvent.

**Graphene oxide**

A processable hole transport layer (HTL) solution for bulk heterojunction organic solar cells (BHJ OSCs) based on varied concentration of graphene oxide (GO) in aqueous suspension has been reported [49]. The freshly prepared GO aqueous solution of varied concentration was spun coated on cleaned, pre-patterned ITO substrate and dried in a nitrogen filled glove box to remove excess solvent. Different concentrations of graphene oxide were investigated and it was observed that at lower concentration of graphene oxide, the PCE of OSC increases as compared to those with higher concentration.

**Other novel materials**

A novel self-assembled quasi-3D nanocomposite has been demonstrated as a p-type hole transport layer [50]. By applying this novel HTL in inverted OSCs covering fullerene and non-fullerene systems, device performance is significantly improved. The champion power conversion efficiency reaches 12.13%, which is the highest reported performance of solution processed HTL based inverted OSCs. The fabrication of the quasi-3D nanocomposite is as shown in Figure 14.

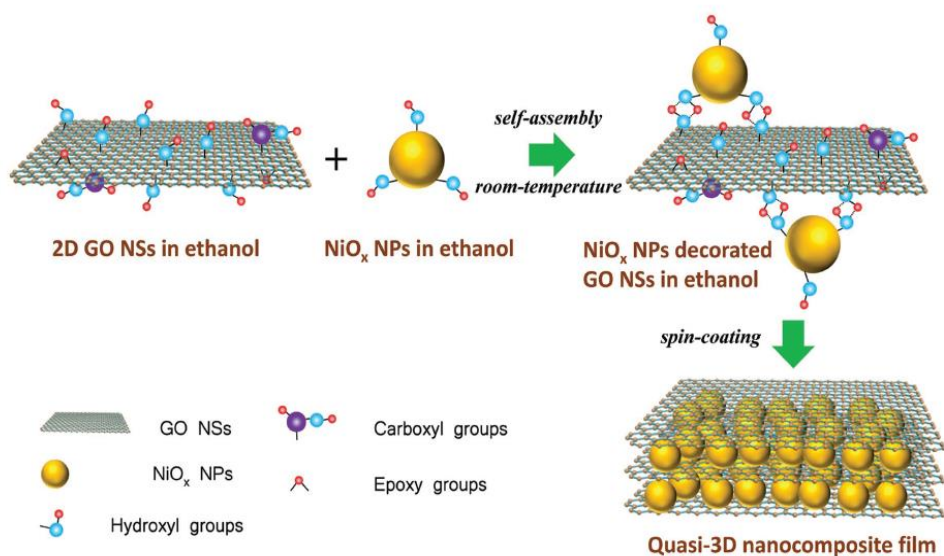


**Figure 14.** Schematic illustration of preparing room-temperature ethanol processed self-assembled quasi-3D GO:NiO nanocomposite

## Conclusion

Based on the reported results in the above presented review and several on-going researches in a bid to increase the dependency on organic solar cells, the engineering of interface materials and the improvement in all other components in OSC are the major target areas to be investigated and improved. Raising the PCE% of organic solar cells would make them a feasible source of environmental friendly and low cost source of energy for future consumption.

## References

- [1] Pulfrey L.D., *Photovoltaic Power Generation*. New York: Van Nostrand Reinhold Co. 1978
- [2] Krebs F.C., Espinosa N., Hosel M., Sondergaard R.R., Jorgensen M. *Adv. Mater.*, 2014, **26**:29
- [3] Huang J., Wang H., Yan K., Zhang X., Chen H., Li C.Z., Yu J. *Adv. Mater.*, 2017, **29**:1606729
- [4] Kong T., Wang H., Liu X., Yu J., Wang C. *IEEE J. Photovolt.*, 2017, **7**:214
- [5] Xing S., Wang H., Kong T., Yu J., Jiang J., Wang C. *IEEE J. Photovolt.*, 2017, **7**:1058
- [6] Ono L.K., Leyden M.R., Wang S., Qi Y. *J. Mater. Chem. A*, 2016, **4**:6693
- [7] Wang Y., Li S., Zhang P., Liu D., Gu X., Sarvari H., Ye Z., Wu J., Wang Z., Chen Z.D. *Nanoscale*, 2016, **8**:19654
- [8] Zhao W., Qian D., Zhang S., Li S., Inganas O., Gao F., Hou J. *Adv. Mater.*, 2016, **28**:4734
- [9] Zhou D., Cheng X., Xu H., Yang H., Liu H., Wu F., Chen L., Chen Y. *J. Mater. Chem. A*, 2016, **4**:18478
- [10] Gil-Escrig L., Momblona C., Sessolo M., Bolink H.J. *J. Mater. Chem. A*, 2016, **4**:3667

- [11] Huang L.B., Su P.Y., Liu J.M., Huang J.F., Chen Y.F., Qin S., Guo J., Xu Y.W., Su C.Y. *J. Power Sourc.*, 2018, **378**:483
- [12] Choy W.C.H., Zhang D. *Small*, 2016, **12**:416
- [13] Walker B., Choi H., Kim J.Y. *Curr. Appl. Phys.*, 2017, **17**:370
- [14] Gollu S.R., Sharma R., Srinivas G., Kundu S., Gupta D. *Org. Electron.*, 2016, **29**:79
- [15] Chueh C.C., Crump M., Jen A.K.Y. *Adv. Funct. Mater.*, 2016, **26**:321
- [16] Zhao W., Li S., Yao H., Zhang S., Zhang Y., Yang B., Hou J. *J. Am. Chem. Soc.*, 2017, **139**:7148
- [17] Kawashima K., Fukuhara T., Suda Y., Suzuki Y., Koganezawa T., Yoshida H., Ohkita H., Osaka I., Takimiya K. *J. Am. Chem. Soc.*, 2016, **138**:10265
- [18] Lee J., Sin D.H., Moon B., Shin J., Kim H.G., Kim M., Cho K. *Energy Environ. Sci.*, 2017, **10**:247
- [19] Huang J., Carpenter J.H., Li C.Z., Yu J.S., Ade H., Jen A.K.Y. *Method. Adv. Mater.*, 2016, **28**:967
- [20] Nian L., Chen Z., Herbst S., Li Q., Yu C., Jiang X., Dong H., Li F., Liu L., Würthner F., Chen J., Xie Z., Ma Y. *Adv. Mater.*, 2016, **28**:7521
- [21] Jin Y., Chen Z., Xiao M., Peng J., Fan B., Ying L., Zhang G., Jiang X.F., Yin Q., Liang Z., Huang F., Cao Y. *Energy Mater.*, 2017, **7**:1700944
- [22] Liu X., Xu R., Duan C., Huang F., Cao Y. *J. Mater. Chem. C*, 2016, **4**:4288
- [23] Li Z., Yang D., Zhao X., Li Z., Zhang T., Wu F., Yang X. *RSC Adv.*, 2016, **6**:101645
- [24] Dong S., Hu Z., Zhang K., Yin Q., Jiang X., Huang F., Cao Y. *Adv. Mater.*, 2017, **29**:1701507
- [25] Bernede J.C., *AIP Conf. Proc.*, 2011, **1391**:9
- [26] Chen D., Zhang C., *Nanostructured Solar Cells (chapter 8: Interface Engineering and Electrode Engineering for Organic Solar Cells)* 2018, pp.161, DOI: 10.5772/65312
- [27] Borse K., Sharma R., Sagar H.P., Pininti A.R., Gupta D., Yella A. *Org. Electron.*, 2016, **41**:280
- [28] Jin F., Su Z., Chu B., Cheng P., Wang J., Zhao H., Gao Y., Yan X., Li W. *Sci. Report.*, 2016, **6**:26262
- [29] Gil-Escrig L., Momblona C., Forgács D., Pla S., Fernández-Lázaro F., Sessolo M., Sastre-Santos A., Bolink H.J. *Org. Electron.*, 2016, **37**:396
- [30] Zheng D., Zhao L., Fan P., Ji R., Yu J. *Nanomaterials*, 2017, **7**:233
- [31] Cao B., He X., Fetterly C.R., Olsen B.C., Lubner E.J., Buriak J.M. *ACS Appl. Mater. Interfaces.*, 2016, **8**:1823
- [32] Chang S.C. *Int. J. Electrochem. Sci.*, 2016, **11**:5819
- [33] Xu W., Yan C., Kan Z., Wang Y., Lai W.Y., Huang W. *ACS Appl. Mater. Interfaces.*, 2016, **8**:14293
- [34] Ullah I., Karim Shah S., Wali S., Hayat K., Khattak S.A., Khan A. *Mater. Res. Expres.*, 2017, **4**:125505
- [35] Xiaodong Li Liu X., Zhang W., Wang H.Q., Fang J. *Chem. Mater.*, 2017, **29**:4176



- [36] Yang Z., Zhang T., Li J., Xue W., Han C., Cheng Y., Qian L., Cao W., Yang Y., Chen S. *Scientific Report.*, 2017, **7**:9571
- [37] Al-hashimi M.K., Kadem B.Y., Hassan A.K. *J. Mater. Sci. Mater. Electron.*, 2018, **29**:7152
- [38] Cho N., *Mol. Cryst. Liquid Cryst.*, 2017, **655**:159
- [39] Upama M.B., Elumalai N.K., Md Mahmud A., Wright M., Wang D., Xu C., Haque F., Chan K.H., Uddin A. *Appl. Surface Sci.*, 2017, **416**:834
- [40] Wu Z., Sun C., Dong S., Jiang X.F., Wu S., Wu H., Yip H.L., Huang F., Cao Y. *J. Am. Chem. Soc.*, 2016, **138**:2004
- [41] Wang J., Lin K., Zhang K., Jiang X.F., Mahmood K., Ying L., Huang F., Cao Y. *Adv. Energy Mater.*, 2016, **6**:1502563
- [42] Wang Z., Zheng N., Zhang W., Yan H., Xie Z., Ma Y., Huang F., Cao Y. *Adv. Energy Mater.*, 2017, **7**:1700232.
- [43] Zhang K., Huang F., Cao Y. *Acta Polym. Sin.*, 2017, **9**:1400
- [44] Xu R., Zhang K., Liu X., Jin Y., Jiang X.F., Xu Q.H., Huang F., Cao Y. *ACS Appl. Mater. Interfaces.*, 2018, **10**:1939
- [45] Chien H.T., Pölzl M., Koller G., Challinger S., Fairbairn C., Baikie I., Kratzer M., Teichert C., Friedel B., *Surfaces Interfaces*, 2017, **6**:72
- [46] Sivakumar G., Pratyusha T., Gupta D., Shen W., *Mater. Today Proceed.*, 2017, **4**:6814
- [47] Wijeyasinghe N., Tsetseris L., Regoutz A., Sit W.Y., Fei Z., Du T., Wang X., McLachlan M.A., Vourlias G., Patsalas P.A., Payne D.J., Heeney M., Anthopoulos T.D. *Adv. Funct. Mater.*, 2018, **28**:1707319
- [48] Beliatas M.J., Helgesen M., García-Valverde R., Corazza M., Roth B., Carlé J.E., Jørgensen M., Krebs F.C., Gevorgyan S.A. *Adv. Eng. Mater.*, 2016, **18**:1494
- [49] Rafique S., Abdullah S.M., Alhummiyany H., Abdel-wahab M.Sh., Iqbal J., Sulaiman K., *J. Phys. Chem. C*, 2017, **121**:140
- [50] Cheng J., Zhang H., Zhao Y., Mao J., Li C., Zhang S., Sing K., Jianhui W., Wallace H., Choy C.H. *Adv. Funct. Mater.*, 2018, **28**:1706403

**How to cite this manuscript:** Oluwatobi O. Amusan, Hitler Louis, Monday Philip, Saud-uz-Zafar, Adejoke T. Hamzat, Ozioma U. Akakuru, Dass M. Peter. Different Interface Engineering in Organic Solar Cells: A Review. *Chemical Methodologies* 3(4), 2019, 425-441. [DOI: 10.22034/chemm.2018.143544.1070](https://doi.org/10.22034/chemm.2018.143544.1070).